Available online at www.sciencedirect.com
ScienceDirect
C. R. Geoscience 339 (2007) 186–199
COMPTES RENDUS GEOSCIENCE
http://france.elsevier.com/direct/CRAS2A/

External geophysics, Climate and Environment

Neoproterozoic glaciomarine and cap dolostone facies of the southwestern Taoudéni Basin (Walidiala Valley, Senegal/Guinea, NW Africa)

Graham A. Shields [a,*], Max Deynoux [b], Stephen J. Culver [c], Martin D. Brasier [d], Pascal Affaton [e], Didier Vandamme [e]

[a] *Geologisch-Paläontologisches Institut und Museum, Universität Münster, Correnstrasse 24, 48149 Münster, Germany*
[b] *École et observatoire des sciences de la Terre, Centre de géochimie de la surface, CNRS–UMR 7517, 1, rue Blessig, 67084 Strasbourg cedex, France*
[c] *Department of Geology, East Carolina University, Greenville, North Carolina 27858, USA*
[d] *Department of Earth Sciences, University of Oxford, Parks Road, Oxford, OX1 3PR, UK*
[e] *CEREGE, CNRS–UMR 6635, université Paul-Cézanne, Aix–Marseille-3, BP 80, Europôle de l'Arbois, 13545 Aix-en-Provence cedex 4, France*

Received 8 February 2005; accepted 3 October 2006
Available online 9 February 2007

Written on invitation of the Editorial Board

Abstract

The Neoproterozoic-age Mali Group of the southwestern Taoudéni Basin, NW Africa, represents, in the Walidiala Valley, a glaciogenic and post-glacial succession that brackets the Cryogenian–Ediacaran period boundary. At its base, debris flows and turbidite-like, sandy units of the Pelel Member pass upward into siltstone and shale of the Diagoma Member. These two units represent the progressive evolution from some portion of a fan delta fed by a nearby ice shelf to a more distal environment disturbed only by the occasional fallout from passing icebergs. The appearance of coarse-grained, cross-bedded sandstone beds and gravels of the overlying Tanagué Member heralds a return to a shallower, fluvially influenced environment before abrupt transgression caps the glaciogenic succession. The transgressive unit consists of a regionally extensive, 2–7 m-thick, silty dolostone, the Bowal Member, which is isotopically and petrographically indistinguishable from ca. 635-Ma cap dolostone units elsewhere in NW Africa and worldwide. The Bowal Member comprises microcrystalline dolomite in turbidite-like depositional sheets disrupted by internal brecciation, fracturing and cementation by first chert and then dolomite. The stratigraphic succession in the Walidiala Valley closely resembles facies models relating to glacial retreat in a proximal glaciomarine environment affected by glacioeustasy. A large volcaniclastic debris flow has caused slumping and soft-sediment deformation within the cap dolostone of the Bowal Member. The widespread association of pyroclastic deposits with cap dolostone throughout the Taoudéni Basin implies that volcanism and deglaciation were roughly contemporaneous across a huge area. We consider that the volcaniclastic debris flow and soft-sediment deformation within the underlying Tanagué Member were possibly triggered by seismic activity during deglaciation, caused by isostatic relaxation of the lithosphere. However, fitted brecciation of cap dolostone beds here and elsewhere in the world is more consistent with pervasive dolomite cementation. ***To cite this article: G.A. Shields et al., C. R. Geoscience 339 (2007).***

* Corresponding author.
E-mail address: gshields@uni-muenster.de (G.A. Shields).

1631-0713/$ – see front matter
doi:10.1016/j.crte.2006.10.002

Résumé

Faciès cap dolostones et glacio-marins néoprotérozoïques dans le Sud-Ouest du bassin Taoudéni (vallée de Walidiala, Sénégal/Guinée, Nord-Ouest de l'Afrique). Dans la vallée de Walidiala, au sud-ouest du bassin de Taoudéni, le groupe du Mali comprend une succession glaciaire et postglaciaire néoprotérozoïque se rapportant à la limite Cryogénien–Édicarien. Cette succession débute par des coulées de débris et turbidites sableuses formant l'unité de Pelel, laquelle passe vers le haut à des *siltstones* et argilites à blocs lâchés de l'unité de Diagoma. Ces deux unités marquent le passage d'un environnement de type lobe deltaïque, proche d'une marge glaciaire, à un environnement plus distal, alimenté notamment par des icebergs. Au-dessus, la présence de grès grossiers à stratifications obliques de l'unité de Tanagué marque le retour à un environnement moins profond et sous influence fluviatile, avant la grande transgression régionale représentée par un banc de 2 à 7 m de dolomies silteuses formant l'unité de Bowal. La composition isotopique et pétrographique de cette unité carbonatée est identique à celle des *cap dolostones* qui coiffent les dépôts glaciaires néoprotérozoïques (∼635 Ma) en Afrique de l'Ouest et ailleurs dans le monde. Il s'agit de dolomie microcristalline formant des lits turbiditiques localement bréchifiés, fracturés, avec un ciment siliceux puis dolomitique. La succession stratigraphique de la vallée de Walidiala est très proche des modèles proposés pour illustrer un retrait glaciaire en milieu marin proximal affecté par la glacio-isostasie. Un important écoulement de débris volcanoclastiques a provoqué glissements et déformations souples dans les bancs dolomitiques de l'unité de Bowal. L'association généralisée de dépôts pyroclastiques avec le dépôt des *cap dolostones* sur l'ensemble du bassin de Taoudéni suggère que les deux phénomènes sont contemporains et en relation avec les événements tectoniques panafricains. On considère que l'écoulement de débris et la bréchification de l'unité de Bowal, ainsi que les déformations souples dans les grès de Tanagué sous-jacents, ont pour origine une activité sismique liée à la relaxation isostatique de la lithosphère lors de la déglaciation ***Pour citer cet article : G.A. Shields et al., C. R. Geoscience 339 (2007).***

Keywords: Neoproterozoic; Glaciation; Senegal; Dolostone; Stable isotopes

Mots clés : Néoprotérozoïque ; Glaciation ; Sénégal ; Dolomite ; Isotopes stables

1. Introduction

Evidence for glaciation during the Neoproterozoic is widespread on Earth and consistent with repeated glaciation between ca. 750 Ma and ca. 580 Ma (Gaskiers) [22]. Of these events, the Elatina–Ghaub–Nantuo glaciation at ca. 635 Ma is the most easily recognized, because deglaciation was associated worldwide with the deposition of a thin, draping dolostone unit displaying knife-sharp, onlapping contact with underlying glaciogenic strata [26]. Cap dolostone units are so distinctive that a cap dolostone overlying glaciogenic diamictite of the Elatina Formation in Australia was chosen to mark the beginning of the newly defined terminal Proterozoic period: the Ediacaran Period (circa 632–542 Ma) [27]. The underlying rationale behind this decision is that cap dolostone units represent a unique depositional event that can be correlated worldwide. In terms of the fossil record the new Ediacaran period encompasses the earliest records of undoubted metazoans [42] as well as the taxonomically enigmatic soft-bodied Ediacaran fauna.

Despite excellent preservation of glacial and periglacial deposits and the existence of an extensively developed Elatina-type cap dolostone [13–15,39], the NW African sections of the Taoudéni Basin (Fig. 1) have played only a minor role in recent Neoproterozoic

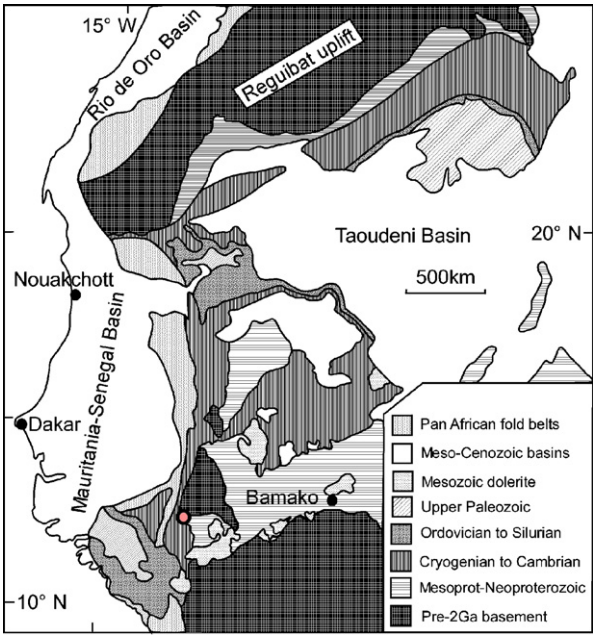

Fig. 1. Geological map of the Taoudéni Basin and adjacent areas in northwestern Africa. Location of Walidiala Valley is indicated by the open circle near the termination of the Mauritanide orogen.

Fig. 1. Carte géologique du bassin de Taoudéni et des régions limitrophes en Afrique de l'Ouest. La localisation de la vallée de Walidiala est indiquée par un cercle en bordure de la chaîne des Mauritanides.

debates, such as those generated by the Snowball Earth Hypothesis [20,21]. This is partly because in contrast to detailed sedimentological studies, geochemical and paleomagnetic investigations have been limited in scope, while fossil-based age constraints remain ambiguous due to the generally barren nature of post-glacial strata. Organic-walled fossils found in units overlying evidence for glaciation in the Volta Basin provide limited support for a Late Neoproterozoic age consistent with an Elatina affinity for the ice age [34]. An Elatina age, i.e. ca. 635 Ma, is also compatible with previously reported Rb/Sr age determinations [8] as well as a recently reported Lu–Hf age of 576 ± 13 Ma [2] for phosphorites that overlie both the cap dolostone and the glacial horizon in the neighboring Volta Basin, which is probably correlative with equivalent strata in the Taoudéni Basin [34]. Confusingly, shelly fossils recovered from a loose block of dolostone in the Walidiala Valley, the subject area of our study, support an Early Cambrian age for the cap dolostone unit (from which the loose block was considered to derive) [11]. These findings have generated calls for a uniquely Early Cambrian glaciation in northwestern Africa [4,16], which on lithological grounds seems to possess all the characteristic features of a Neoproterozoic, or more specifically Elatina age, glaciation [21].

Here we report the findings of a recent field excursion to the Walidiala Valley in January 2002 by GS, MD, PA and DV, and compare these results with published work. In addition, previously unpublished (MB and SC) and new stable isotopic data are presented. New interpretations of the depositional environments of both the glaciogenic strata and the cap dolostone are given below that allow us to reassess the global stratigraphic affinity of the Mali Group of the Walidiala Valley in the light of recent advances in our knowledge of Neoproterozoic events and glacial sedimentology. We examine likely interrelationships between glacioisostasy and the vertical succession of glaciogenic facies. In addition, we address the possible effects of deglaciation and related lithospheric isostatic rebound on regional tectonism.

2. Geological setting

The Taoudéni Basin forms the sedimentary cover of the West African craton (Fig. 1), which has been a coherent, tectonic entity for over 1600 million years. This cover forms a thin (3000 m on average) blanket over the basin, which spans almost 1500 km in diameter, covering 2 000 000 km^2 (Fig. 1). Panafrican to Hercynian orogenic belts surround the basin on all sides but most of the sedimentary cover is devoid of tectonism and metamorphism. Sedimentation in the basin began at around 1000 Ma and had ceased by the Carboniferous Period. Three supergroups have been identified throughout the basin [39] with Supergroup 2 covering the Late Neoproterozoic to Early Ordovician. In the Walidiala Valley, which straddles the Guinea–Senegal border in the extreme southwestern Taoudéni Basin, supergroups 1 and 2 overlie basement rocks of the Kenieba Inlier and are intruded and protected from erosion by plateau-forming diabase sills of Jurassic age. Supergroup 1 consists of intertidal to supratidal, coarse-grained, red wackestones and intervening siltstone forming the so-called Segou Group. In the region of study, the lower part of Supergroup 2 is represented forming the Mali Group [3,40], which rests on the Segou Group with deep erosional unconformity. The Mali Group consists of siliciclastic, mostly siltstone units and comprises in its basal part the regionally correlative 'triad' [39,43] of glaciogenic diamictite, dolostone, and bedded chert.

Palaeogeographic reconstructions of the 'triad'-associated glaciation of northwestern Africa [13,14] envisage an ice sheet centered towards the North of the Reguibat Shield (Fig. 1) with inferred glacial movement southward on the platform and laterally toward oceanic troughs or basins located at the present position of the Panafrican belts. Accordingly, continental glaciation is recorded in correlative strata of the northern part of the Taoudéni Basin by a thin, irregular (0 to 50 m thick) veneer of terrestrial tillites with subordinate proglacial outwash deposits preserved in limited shallow depressions. Towards the South of the platform, the glacial drift thickens (150–200 m) and comprises marine deposits in small intracratonic basins in western Mali (Kayes area) or at the margins of oceanic troughs bordering the Panafrican Bassaride Belt in eastern Senegal and Guinea. This study focuses on the latter areas, where glacial deposits have been described as shallow marine and ice-proximal [9,10].

3. Lithostratigraphy of the Mali Group in the Walidiala Valley

According to Culver and Hunt [10], the Mali Group can be subdivided into two formations (Fig. 2): the Hassanah Diallo Formation, 50–120 m thick, which represents the glacially related deposits, and the Nandoumari Formation, up to 130 m thick, which comprises at its base quartz arenites overlain by dolostone, siltstone and bedded chert.

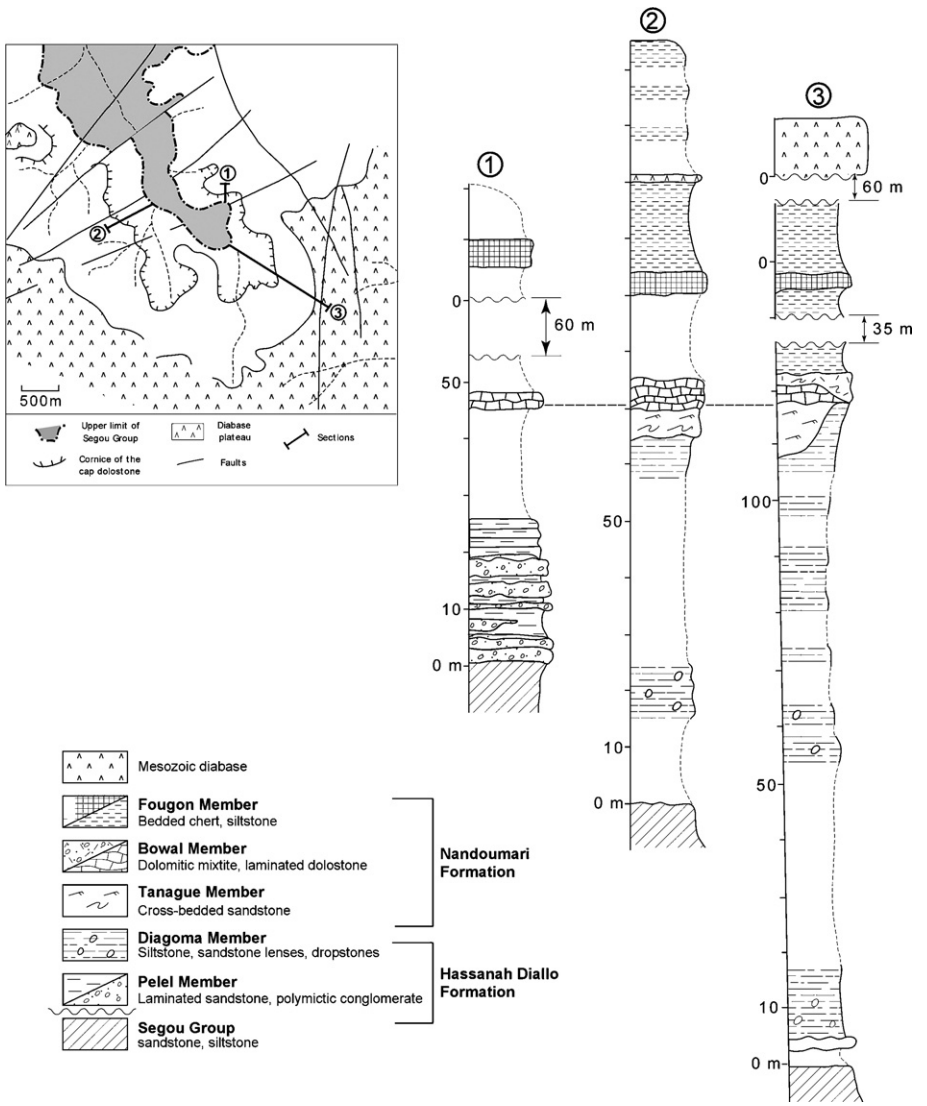

Fig. 2. Three measured sections of the Mali Group in the Walidiala Valley; section 2 is roughly equivalent to NSF5-22-89 [24] and section 3 to NSF5-23-89 [24]. Aerial photo (No. 137) interpretation is shown in inset.

Fig. 2. Trois coupes du groupe du Mali dans la vallée de Walidiala. La coupe 2 est grossièrement équivalente à NSFS-22-89 [24] et la coupe 3 à NSFS-23-89 [24]. En médaillon, schéma interprétatif d'après une photo aérienne (n° 137).

3.1. Hassanah Diallo Formation

The Pelel Member, which forms the lower part of the Hassanah Diallo Formation, consists of 0–35 m of massive clast- to matrix-supported pebble-boulder conglomerate alternating with fine- to coarse-grained laminated sandstone.

The conglomeratic horizons, 0.5–2 m thick, display polymictic clasts of various size (up to 2.5 m in the lowermost conglomerate) and shape (angular to well rounded), randomly oriented in a variously distributed matrix made up of an unsorted mixture of small pebbles, granules, and coarse sand (Fig. 3a). Rare clast imbrications occur (Fig. 3b). A crude to well-defined upward decrease in clast sizes is generally visible in each conglomeratic horizon (Fig. 3a–c), which are locally capped by a decimeter-thick bed of well sorted, coarse-grained sandstone (Fig. 3b). The contact of the conglomeratic horizons on the intervening laminated sandstone is sharp, slightly erosive (Fig. 3c), and locally disturbed by loading of overlying large clasts (Fig. 3d).

The intervening sandstone unit, a few decimeters up to two meters thick, consists either of fine-grained

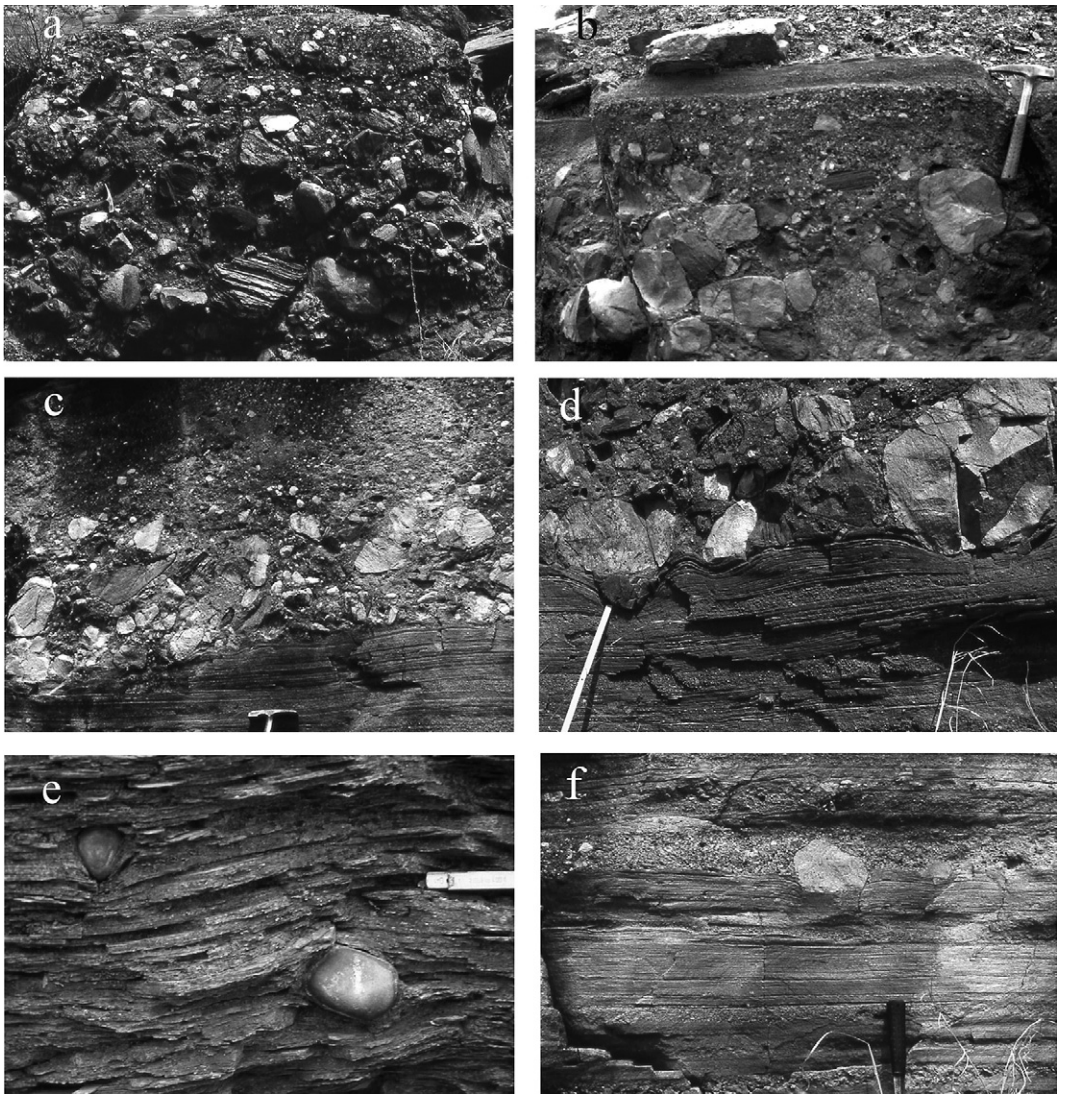

Fig. 3. Facies of the conglomeratic horizons and intervening sandstone of the Pelel Member. (**a**) Clast- to matrix-supported conglomeratic horizon with polymictic clasts of various shape and sizes including angular pebbles from the underlying Segou Group. (**b**) Conglomeratic horizon showing clast imbrications (lower left), fining upward trend and a well-sorted sandstone cap. (**c**) Slightly erosional contact between a well-defined fining upward conglomeratic horizon and the underlying interval of laminated sandstone. (**d**) Loading disturbance at the contact between a conglomeratic horizon and intervening coarse-grained laminated sandstone including centimeters thick granule sandstone intercalations. (**e**) Wavy laminated fine-grained sandstone disrupted by outsized lonestones in a sandstone interval. (**f**) Sandstone interval showing centimeter-thick flat, normally graded lamination of medium-grained sandstone and intervening granule-size gravel layers, including a small outsized clast.

Fig. 3. Faciès des horizons conglomératiques et grès intercalés de l'unité de Pelel. (**a**) Horizon conglomératique à galets polygéniques jointifs ou non, aux formes variées et comprenant notamment des galets anguleux du groupe de Ségou sous-jacent. (**b**) Horizon conglomératique granoclassé à galets imbriqués (partie inférieure gauche), coiffé par un niveau gréseux bien trié. (**c**) Contact légèrement érosif entre un horizon conglomératique à granoclassement normal et un niveau de grès laminé sous-jacent. (**d**) Figure de charge au contact entre un horizon conglomératique et une intercalation de grès grossier laminé comprenant des passées centimétriques à granules. (**e**) Grès fin à galets lâchés et laminations ondulées. (**f**) Intercalation de grès moyen à laminations centimétriques planes, granoclassées et passée graveleuse comprenant notamment un gros galet.

sandstone with thin wavy laminations locally disrupted by rare out-sized lonestones (Fig. 3e), or of centimeter-thick, flat, normally graded laminations of medium-grained sandstone including repetitive intercalations of gravelly sandstone with locally larger clasts (Fig. 3f). The contact of these sandy intervals with the underlying conglomerate appears either as a sharp lithologic change (conglomerate to wavy laminated fine-grained sandstone), or is gradational (conglomerate to flat laminated, medium- to coarse-grained sandstone).

Most of the above observations were made in section 1 (Fig. 2), where the vertical succession of the Pelel Member is fully exposed and can be traced laterally over 50 to 100 m, allowing observation of the sheet-like geometry of the conglomerate and intervening sandstone unit. In this section, angular reddish sandstone clasts from the Segou Group are prominent in the lowermost conglomeratic horizons, but become less abundant upward relative to extrabasinal clasts including basement rocks. The uppermost conglomeratic horizon displays slump structures and is overlain by eight meters of well bedded, fine-to medium-grained sandstone, horizontally laminated or displaying tabular cross bedding and current ripples.

The conglomeratic succession of the Pelel Member is generally poorly exposed and could be wholly absent in some parts of the valley. Where present it passes conformably up into the Diagoma Member of laminated siltstone interspersed with centimeter- to decimeter-thick, fine- to medium-grained, normally graded sandstone beds that become less abundant up section. The Diagoma Member siltstone unit is greenish brown, finely laminated, with ripples visible in places, and contains rare lonestones at various levels. These lonestones are well rounded, up to 20 cm in diameter, and consist of fine-grained quartzite and rare basement rocks. They are mainly found in the lower parts of the siltstone succession and have been considered entirely absent from the uppermost parts (at least 15 m) of the Diagoma Member [10].

3.2. *Nandoumari Formation*

Olive green siltstone of the Hassanah Diallo Formation is overlain with erosional unconformity by up to 10 m of pinkish to greenish grey, decimeter-bedded, well-rounded quartz arenite sandstone and gravel-sized conglomerate of the Tanagué Member. These form a series of prominent but discontinuous cliffs around the Walidiala Valley, and were regarded as possible channel structures [10]. Internally, sandstone beds are typically cross-bedded, with granule-size clasts lining the foresets. They are locally folded by soft-sediment deformation that can be related to slumping, loading, or liquefaction.

The overlying unit, the Bowal Member dolostone, overlies sharply either the sands and gravels of the Tanagué Member or siltstone of the Diagoma Member. Two lithofacies can be distinguished within the Bowal Member dolostone: lithofacies I, which is a microcrystalline, laminated dolostone (Fig. 4a), and lithofacies II, which is a dark, dolomitic diamictite unit (Fig. 4b). Lithofacies I forms cm-dm bedded, internally laminated dolostone and dolomitic siltstone beds, and is petrographically similar to cap dolostone facies in other parts of the Taoudéni Basin, as well as in the Australian central superbasin [26] and elsewhere in the world [23]. Accordingly, lithofacies I is characterized by various forms of brittle deformation: fractures, tepee-like buckling and discontinuous fitted brecciation [32] with created space being filled either by early chert and/or by dolospar. In relatively undeformed beds, this fine-grained dolostone exhibits mm-scale layering defined by mechanical laminations with no textural evidence for any microbial influence, see [10]. Microscopically, lithofacies I uniformly comprises equigranular grains of dolomite (generally $>90\%$) with accessory quartz and biotite grains of similar size. Individual beds have sharp or erosional bases and fine upwards from a surface of detrital dolomite/quartz lag of roughly 100 micron-size to dolomicrite of <10 μm in diameter, which has been described elsewhere as turbidite-like [26]. Most beds do not exhibit the entire range of grain-sizes due to scouring. Micritic parts are associated with pyrite, which commonly forms <1-mm-sized cubes.

On the eastern side of the Walidiala Valley, the Bowal Member is thicker, in places up to 7 m (Fig. 4a), and contains within it a diamictite facies (lithofacies II). Lithofacies II is generally found as matrix-supported, homogenized packages of coarse-grained diamictite debris up to several meters in height (Fig. 4b) that has pushed against and scoured into beds of lithofacies I, leading to massive slumping and soft-sediment deformation and buckling (Fig. 4a and c). The dark, speckly, and massive appearance of lithofacies II stands out clearly against the buff-colored, stratified units of lithofacies I (Fig. 4d). Diamictite clasts range in size from sub-millimeter to decimeter-scale with the largest, a 70-cm-diameter rounded granitoid boulder. Other rock types present as large decimeter-scale clasts include sandstone (Fig. 4d), quartzite and limestone.

On the microscopic scale, clasts are dominated by well-rounded to angular quartz and feldspar as well as rounded pellets of a finely crystalline, but altered igneous rock of possibly andesitic composition, comprising mostly plagioclase feldspar, long, thin laths of muscovite and chlorite. The diamictite matrix is similar in appearance to these pellets, and both have reverted consistently to muscovite mica and chlorite in all samples, hence its dark color. Idiotopic dolomite rhombs up to a millimeter in size have grown in this largely chloritic matrix in all samples of lithofacies II (Fig. 4e and f), lending it a characteristic speckled appearance. Mica crystals commonly wrap around

Fig. 4. Facies of the dolostone Bowal Member. (**a**) Conformable layers of laminated dolostone of lithofacies I underlie dolostone beds disrupted and brecciated by slumping from right to left. Triangular brecciated area has been infilled by early chert. Height of photo = 1 m. (**b**) Dark wall of lithofacies II diamictite. (**c**) Folding and slumping of cap dolostone downslope from right to left. (**d**) Silicified contact between dolostone of lithofacies I (below) and diamictite of lithofacies II (above). (**e**,**f**) Photomicrographs of diamictite facies (lithofacies II) in plane polarized light (**e**) and crossed polars (**f**) showing greenish brown chlorite, muscovite and albite-rich matrix (left) replaced in part by authigenic dolomite rhombs (right and centre). Irregular patch below central dolomite rhomb shows late replacement by calcite. Field of view is 2.8 mm across.

Fig. 4. Faciès des dolomies de l'unité de Bowal. (**a**) Lits concordants de dolomie laminée du lithofaciès I, surmontés par des lits déformés et bréchifiés par suite de glissements orientés de la droite vers la gauche du cliché. La zone triangulaire bréchifiée a été infiltrée par des silicifications précoces Hauteur de la photo = 1 m. (**b**) Paroi sombre de diamictite du lithofaciès II. (**c**) Plissements et glissements des *cap dolostones* selon une pente orientée vers la gauche du cliché. (**d**) Contact silicifié entre les dolomies du lithofaciès II (en haut). (**e**,**f**) Microphotos des diacmitites du lithofaciès II en lumière polarisée dans un plan (**e**) et (**f**), montrant une matrice brun vert riche en chlorite, muscovite et albite (partie gauche) partiellement remplacée (partie droite et centrale) par des rhomboèdres de dolomite authigéniques. Sous le rhomboèdre central, une plage irrégulière correspond à un ultime remplacement par de la calcite. Le champ de chaque cliché correspond à 2,8 mm.

isolated dolomite rhombs, indicating that dolomitisation took place in situ. Indeed, dolomite replaces plagioclase widely, while accessory calcite fills sporadic remnant voids only.

Although this diamictite facies is not obvious in outcrops on the western side of the Walidiala Valley, an equivalent coarse-grained unit has been identified, which scours into and fills cavities within laminated beds of lithofacies I. Only one sample (#09/01/02.4) was collected of lithofacies II from the western side. This clast-supported facies comprises rounded quartz sand and gravel grains together with perfectly euhedral dolomite crystals, identical to those from lithofacies II, but which have here been reworked as clasts.

Chert is ubiquitous in cap dolostone outcrops on both sides of the Walidiala Valley, filling fractures (Fig. 4a), enveloping breccia clasts of lithofacies I and exploiting cavities along bedding planes. Chert defines the contact between lithofacies I and II (Fig. 4d) and formed contemporaneously with the dolomite: later than the fitted brecciation of dolomite beds but more-or-less contemporaneous with later cementation by dolomite. In places it can be seen that chert veins issue from the diamictite facies forming chalcedony geodes in voids.

Greenish siltstone beds of the overlying Fougon Member show no signs of soft-sediment deformation and drape conformably the uppermost beds of the cap

dolostone unit, onlapping the relief caused by the slumping of the Bowal Member.

4. Stable isotope study

Bulk carbonate samples of the Bowal Member cap dolostone were collected by D. Hunt and S. Culver in 1989 for stable isotope analysis, which was carried out at the University of Oxford during the early 1990s, but remained unpublished. Samples were first cleaned with H_2O_2 and $(CH_3)_2CO$ and dried for 30 min at 60 °C before reaction with anhydrous phosphoric acid at 90 °C. Delta values are reported relative to the international PDB standard.

Three sections [12] were sampled from both sides of the Walidiala Valley: NSF5-22-89 (western side) and NSF5-23-89a and NSF5-23-89b (eastern side), the last two of which are only 30 metres apart. These two successions roughly correspond to our sections 2 and 3, respectively (Fig. 2). The cap dolostone unit was 6.5 m thick in section NSF5-22-89 and only 2 m thick in section NSF5-23-89a, approximately half of which comprised decimeter-scale dolostone beds with the other half being more siliciclastic, dolosilt units of similar dimensions. The cap dolostone in the neighboring section NSF5-23-89b was thicker at 3.7 m, although its base was not observed. All samples were apparently of lithofacies I, although lithofacies II was not recognized in earlier studies.

Additional bulk carbonate samples (Table 1) were collected by GS in 2002 and prepared for analysis in 2005 at the University of Saskatchewan, Canada, by Tim Prokopiuk. Samples were roasted in a vacuum oven for 1 h at 200 °C to remove water and volatile organic contaminants before reaction with anhydrous phosphoric acid at 70 °C. Isotope ratios were corrected for acid fractionation and are reported relative to the international V-PDB standard. Standard deviations for $\delta^{13}C$ and $\delta^{18}O$ are 0.05 ‰ and 0.10 ‰, respectively. All sample data are reported as calcite

Table 1
Stable isotope compositions of cap dolostones of the Walidiala Valley, Senegal/Guinea. Samples 10/01/02.1–4 derive from a fallen block. Height refers to height above base of cap dolostone in all cases. W/E refers to whether the samples derive from the western (W) or eastern (E) sides of the Walidiala Valley

Tableau 1
Composition isotopique des *cap dolostones* de la vallée de Walidiala (Sénégal–Guinée). Les échantillons 10/01/02.1–4 proviennent d'un bloc tombé. Dans tous las cas, la hauteur est donnée par référence à la base des *cap dolostones*. W/E indique la provenance occidentale ou orientale des échantillons par rapport à l'axe de la vallée de Walidiala

Sample	W/E	Height m	$\partial^{13}C$ ‰	$\partial^{18}C$ ‰	Sample	W/E	Description	Height m	$\partial^{13}C$ ‰	$\partial^{18}C$ ‰
Con1	E	0.00	−4.0	−6.4	DH1o	W		3.56	−4.7	−6.1
Con2	E	0.09	−6.4	−7.8	DH1p	W		4.20	−4.6	−6.9
Con3	E	0.28	−2.8	−4.9						
Con4	E	0.38	−3.8	−6.1						
Con5	E	0.56	−3.3	−5.8	11/01/2002	E	diamicite dolospar	-	−3.7	−4.5
Con6	E	0.60	−2.9	−4.7	11/01/02.7	E	diamicite dolospar	-	−4.3	−6.5
Con7	E	0.71	−3.4	−5.8	09/01/02.4	W	diamicite dolospar	-	−3.8	−5.5
Con8	E	0.82	−2.6	−4.9	11/01/02.6	E	diamicite dolospar	-	−4.4	−5.4
Con9	E	0.90	−2.9	−5.3	11/01/02.5A	E	diamicite dolospar	-	−4.3	−6.0
Con11	E	1.30	−3.1	−4.7	11/01/02.5B	E	diamicite dolospar	-	−4.4	−5.8
Con12	E	1.88	−5.1	−6.1	10/01/02.7	E	dolomicrospar	0.1	−3.7	−6.5
WC2	E	0.47	−2.8	−5.7	10/01/02.8	E	dolomicrospar	0.6	−3.2	−6.3
WC3	E	1.13	−2.7	−5.4	10/01/02.9	E	dolomicrospar	1.1	−3.8	−6.7
WC4	E	1.91	−2.8	−5.4	10/01/02.10	E	dolomicrospar	1.6	−3.7	−6.4
WC5	E	2.16	−2.3	−4.3	10/01/02.11	E	dolomicrospar	2.1	−3.5	−6.7
WC6	E	2.25	−4.0	−6.7	10/01/02.12	E	dolomicrospar	3.1	−3.8	−5.9
WC7	E	2.63	−3.3	−7.6	10/01/02.13	E	dolomicrospar	3.3	−3.9	−5.9
WC8	E	3.09	−3.0	−6.5	10/01/02.14	E	dolomicrospar	3.8	−4.7	−7.3
DH1c	W	0.25	−3.3	−6.7						
DH1i	W	0.30	−2.7	−6.1	10/01/02.1	E	dolomicrospar	0.2	−4.2	−7.2
DH1h	W	0.44	−4.2	−6.7	10/01/02.2	E	dolomicrospar	2.0	−3.5	−6.4
DH1e	W	0.80	−4.3	−6.6	10/01/02.4	E	fissure fill dolospar	3.0	−4.8	−7.5
DH1e	W	0.80	−4.0	−6.1	10/01/02.3	E	fissure fill dolospar	4.5	−8.3	−7.9
DH1j	W	1.44	−4.5	−6.5						
DH1m	W	1.94	−4.0	−6.4	10/01/02.3	E	dolospar from cap top	4.0	−8.3	−7.9
DH1n	W	3.00	−4.0	−6.9	11/.1/02.1	E	dolospar from cap top	4.0	−3.0	−7.8

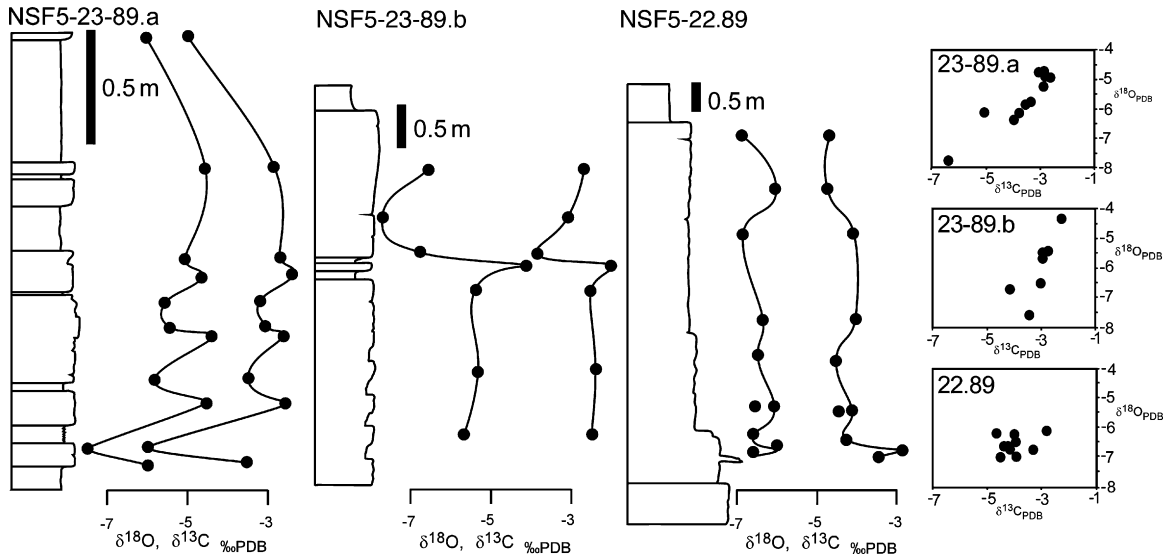

Fig. 5. Stable-isotope profiles from the Walidiala Valley cap dolostone with $\delta^{13}C/\delta^{18}O$ crossplots inset. Isotope profiles begin at first dolostone bed in each case. No lithological information is shown because the key to the original 1989 stratigraphic logs has been lost. NSF5-22-89 yields the most consistent data and does not exhibit covariation.

Fig. 5. Profils des isotopes stables des *cap dolostones* de la vallée de Walidiala, avec en encart les pointages comparatifs $\delta^{13}C/\delta^{18}O$. Les profils isotopiques débutent, dans chaque cas, avec le premier banc de dolomie. Aucune indication lithologique n'est donnée, en raison de la perte des logs stratigraphiques originaux de 1989. L'échantillon NSFS-22-89 fournit les données les plus logiques et ne montre pas de covariance.

although their mineralogy was pure dolomite (<5 % calcite).

Carbon isotope values (Fig. 5; Table 1) from the Walidiala Valley cap dolostone are consistently negative, ranging between −6.4 ‰ and −2.3 ‰, averaging −3.7 ‰ ($n = 42$). Oxygen isotope values for the same samples range between −7.8 ‰ and −4.3 ‰, averaging −6.1 ‰ ($n = 42$). (Six samples of dolospar from highly brecciated levels within the cap are not included in the above statistics.) In general, the data show positive covariance of $\delta^{13}C$ and $\delta^{18}O$ (Fig. 5), which is a commonly used [25] but possibly misleading indicator of diagenetic alteration [29]. Covariation is less apparent in the data from the western section NSF5-22-89 (Fig. 5), which is relatively unaffected by brittle deformation and veining, and is most apparent in four samples from a fallen block of brecciated dolostone, for which sparry dolomite in fissures was specifically selected for analysis, and for two samples from the heavily veined and brecciated cap dolostone top (Table 1). By contrast to the other localities, section NSF-22-89 exhibits limited variation in $\delta^{18}O$ with an overall range of less than 1 ‰ (−6.9 ‰ to −6.0 ‰) associated with falling $\delta^{13}C$ values from −2.7 ‰ to −4.6 ‰. These absolute isotopic values and $\delta^{13}C$ trend are indistinguishable from published stable isotope results from possibly correlative cap dolostone units of the neighboring Volta Basin of Burkina Faso [34].

Dolospar from diamictite facies on both sides of the valley yielded highly consistent results, averaging −4.2 ‰ and −5.6 ‰ for $\delta^{13}C$ and $\delta^{18}O$, respectively. $\delta^{13}C$ values from these purely diagenetic samples are consistent with data from the two possibly altered sections and the lowermost values from section NSF-22-89. The generally consistent $\delta^{18}O$ values for cap dolostone units across NW Africa (with the exception of late-stage dolospar filling fissures) are indicative of a unique source for all carbonate ions, most likely contemporaneous seawater, and imply that no significant differences in fluid temperature were experienced during deposition and early diagenesis.

Two samples of lithofacies II were analyzed commercially at Antellis SARL in Toulouse, France, for their Sr isotope compositions, yielding highly radiogenic values of 0.712870 and 0.719835. Analyses during the same sample run of the standard NBS SRM987 gave expected values of 0.710243 ($n = 2$). Samples were prepared by first preleaching in 80 % acetic acid at room temperature for 24 h, followed by thorough rinsing in ultrapure water, then dissolution in 80 % acetic acid at 90 °C over 24 h. This procedure was conceived in order to first dissolve accessory calcite, before partially dissolving the dolomite rhombs without significantly leaching Sr from clay and other silicate minerals. Such radiogenic values reflect the Rb- and clay-rich nature of this lithology. As such, they are unlikely to

convey the Sr isotopic signature of contemporaneous seawater and are not discussed further.

5. Discussion

5.1. Elatina age of the Walidiala Valley glaciation and cap dolostone

Equally thin (4–10 m) and petrographically similar cap dolostone from post-Elatina sections of the Adelaide geosyncline, the Amadeus and Ngalia basins and the Kimberley Regions of Australia have been analyzed with identical $\delta^{13}C$ results, ranging between −6.3 ‰ and −2.1 ‰, and averaging −3.8 ‰ [26]. $\delta^{13}C$:$\delta^{18}O$ covariation is also apparent in Australia, with a general trend towards lower $\delta^{13}C$ up-section [26]. The authigenic precipitation of barite during late stages of cap deposition is another feature common to both the Taoudéni Basin, although not in its southwestern corner, and Australian basins. Considering the overall similarity between the Taoudéni Basin succession and Elatina successions of Australia in terms of sedimentology, petrography, and C-isotope compositions and trends, it is difficult to avoid the conclusion that the processes involved in the formation of these cap dolostone units are intimately related and that they are likely to be of the same age, i.e. ca. 635 Ma [1]. In [34], similar conclusions were reached with regard to the neighboring and probably correlative Volta Basin 'triad' succession.

Considering the increasing likelihood that the Taoudéni Basin triad is Neoproterozoic in age, it is important to address the apparent anomaly of Cambrian-type shelly fossils in the Walidiala Valley cap dolostone [11]. The presence of *Aldanella attleborensis*, an early gastropod, implies an Early Cambrian age for the cap dolostone, and has been used to constrain the age of agglutinated foraminifera recovered from siltstone of the overlying Fougon Member [12] as well as of glacial events throughout NW Africa [4,16]. Agglutinated foraminifera are tentatively reported from Ediacaran strata in South America [18], while their presence in the Neoproterozoic is to be expected from molecular studies [33]. Therefore, the presence of foraminifera in overlying strata is equally compatible with both a Cambrian and a Neoproterozoic age for the NW African glaciation and its associated cap dolostone. Further investigations of dolostone outcrop samples have failed to come up with additional phosphatic shelly fossils [12], which permits the possibility that the loose block of dolostone from which the fossils were recovered did not derive from the cap dolostone. This is supported by the phosphatized nature of the small shelly fossils [11] against the total absence of phosphate in our thin-sections of the Walidiala Valley cap dolostone. With this in mind, it seems unwise to use the shelly fossils of the southeastern Taoudéni Basin to constrain the age of that succession [34]. Molecular phylogenetic studies that reconstruct the evolutionary relationships between early skeletal organisms such as foraminifera [18] and mollusks need to bear this in mind.

5.2. Facies interpretation

The basal conglomeratic facies of the Hassanah Diallo Formation was considered originally on the basis of *laminations and flow structures*, to relate to *diamictite (tillite)* deposited in a *shallow marine depositional environment at the base of or in front of a partially grounded ice sheet* [9,10]. The sheet-like bed geometry of the conglomeratic horizons, the clast- to matrix-supported texture, the crudely coarse tail normal grading, the occasional presence of clast imbrications, and the absence of muddy material suggest subaqueous, cohesionless debris flows [28,31,35] with occasionally preserved waning flow sand horizons at their tops [17]. The flat laminations and microconglomeratic stringers of the intervening sandstone unit correspond to a high-energy, turbulent flow characteristic of a sandy, high-density turbidity current [28] or concentrated density flow. Accordingly, the Pelel Member could represent the proximal portion of a fan delta.

The tabular to cross-bedded and rippled gravelly sandstone that overlies the conglomeratic succession of the Pelel Member marks the passage to a more quiescent environment illustrated by the deposition of siltstone of the Diagoma Member. This transition to siltstone, disrupted only by occasional lonestones, and then to finely laminated, but otherwise featureless siltstone and shale suggests that the depositional regime became increasingly distal with time and that the supply of terrigenous debris gradually dissipated. No striated or faceted clasts have been recognized either within the conglomeratic horizons or as lonestones, which suggests that the clasts did not originate directly from a grounded glacier or ice shelf. The angular and unworn nature of basinal clasts from the Segou Group, and the rounded shape of most exotic clasts implies a localized and riverine (perhaps fluvio-glacial) rather than sub-glacial origin. By contrast, diamictite clasts from more northern parts of the Taoudéni Basin are commonly faceted and striated, which is consistent with their proximity to terrestrial, periglacial environments and evidence for grounded ice [13].

Sandstone and conglomerate of the Tanagué Member may correspond to fluvial streams, as previously proposed [10], or at least to fluvially dominated shallow marine deposits (delta) when sea-level was temporarily lower, presumably caused by the onset of regional deglaciation and related isostatic rebound. We note that the entire glaciogenic succession of the Walidiala Valley, which consists of debris flows and associated turbidite-like deposits (Pelel Member), passing into progressively more distal, well-laminated siltstone and shale with dropstones becoming rarer upward (Diagoma Member), and in turn unconformably overlain by fluvial sandstone (Tanagué Member), resembles the models dealing with glacial retreat in a proximal glaciomarine environment affected by continuing basin subsidence and glacioisostasy [7]. Additional studies of more regional scope are required to confirm this facies model.

The turbidite-like event horizons within the dolostone and the grain-size grading of the dolomite grains of lithofacies I (Bowal Member) point to a detrital, subaqueous or marine origin for much of the dolomite, and confirm that the cap unit marks a sharp, but apparently conformable transgressive surface. It is possible that the cap dolostone represents the early stages of a major transgression, related to a final, more widespread and possibly global melting episode, which appears to have followed or outpaced regional isostatic rebound. The very fine-grained nature of some of the dolomite implies that dolomite precipitated first as powder, possibly in the water column of the surface mixed layer, and subsequently experienced sea-floor winnowing together with same-sized terrigenous detritus before deposition and cementation. It is difficult to determine whether dolomite was the primary carbonate precipitate but this cannot be ruled out. By contrast, the displacive growth of larger (< 1 mm) dolomite crystals within the diamictite matrix speaks for substantial precipitation (cementation) of primary dolomite during early diagenesis within the sediment, in cases almost entirely replacing the original sediment. Alternatively, this dolomite may have derived originally from mixing with the dolostone during slumping.

The matrix supported framework, randomly dispersed outsized clasts and massive texture of lithofacies II suggest that the deposit had a high density and high cohesive strength, which further imply that the material was deposited *en-masse* in the form of a cohesive debris flow deposit. However, debris flows generally display sheet-like morphology and do not erode to any significant extent the underlying deposits [30,31]. The scouring relationship between lithofacies I and II can be accounted for by a slumping event that took place shortly after the debris flow struck. This interpretation is supported by the observation that cap dolostone beds of lithofacies I that are adjacent to or below lithofacies II are characterized by soft-sediment deformation, such as slumping, mini-normal faults within beds, folding, brecciation at fold hinges and homogenization (possible liquefaction) of normally laminated beds. It seems plausible that the uneven relief of the cap dolostone caused by the underlying sandstone knolls of the Tanagué Member contributed in large part to the folding and compression of dolostone strata downslope (Fig. 4). The exotic, volcanogenic nature of the diamictite matrix and associated pellet-like clasts point to the diamictite matrix's origin as a volcaniclastic deposit, which was subsequently caught up in a massive debris flow triggered by slope failure, possibly due to volcanically induced seismicity or simple loading of the fallout debris. The timing and distribution of chert, emanating as veins from lithofacies II, and commonly exploiting the contact between lithofacies I and II, are consistent with extensive mobilization of silica during early alteration of the volcanogenic material accompanied by pervasive replacement and cementation by dolomite.

5.3. Cap dolostone deformation and disruption

Deformation features are almost ubiquitous within the Walidiala Valley cap dolostone and correlative units across NW Africa and are of both brittle and ductile or 'soft-sediment' origin. Brecciation is common throughout the cap dolostone, forming fractures, cavities and fitted-breccia layers, but is absent from both lithofacies II and the overlying siltstone. Fitted brecciation has been described from elsewhere in the Taoudéni Basin [6,14] and the world [26,32], but its genesis remains enigmatic. In the case of the Walidiala Valley cap dolostone, an evaporitic origin for these features seems unlikely due to the lack of other indicators for shallow marine conditions, the absence of any evaporite mineral pseudomorphs, and the clearly transgressive nature of the cap dolostone. The presence of such a substantial debris flow within the cap dolostone also speaks for a deeper, possibly subtidal marine environment at least for the upper parts of the unit.

Another possibility is that fissures and fitted brecciation formed through seismic activity as argued by [32], in which a strong case was made that cap dolostone deformation on the Brazilian Amazon Craton was related to isostatic rebound-associated relaxing of the lithosphere caused by rapid deglaciation. This interpretation could also be applied to the Walidiala

Valley cap dolostone because of its inferred deposition during deglaciation and lithospheric rebound, indicated by the transient return to shallow water conditions marked by the Tanagué Member sandstone. The convoluted bedding observed within the Tanagué Member is not associated with the incoming debris flow and so may indeed have been related to rebound-related seismicity; however, slumping within the cap dolostone does not require a seismic origin because it can be explained adequately by the arrival of a massive debris flow.

Similarly, although we cannot rule out that seismicity was the cause of some of the brittle deformation and brecciation in the Walidiala Valley cap dolostone, the ubiquitous presence, lateral extent and characteristic fitted texture of cap dolostone disruption imply that its presence is not only of regional significance but is inherent to the cap dolostone formation process. Early cementation by dolomite is obvious in both lithofacies I and II, and in many cap dolostones worldwide, which suggests an unusually high degree of dolomite supersaturation during early diagenesis that would necessarily have caused buckling and brecciation. The greatly oversaturated nature of the post-glacial ocean has been widely noted and continues to be the source of much speculation [20,21]; this aspect is discussed in more length in Section 5.4.

Elsewhere in the Taoudéni Basin, volcanogenic chert and volcaniclastic material are also found at the top of the cap dolostone, while convoluted bedding is common even in the absence of debris flows [6,14]. Therefore, it is conceivable that regional volcanism and associated seismicity were widespread after glaciation, possibly triggered by glacioisostatic relaxation of the lithosphere. During the Quaternary Period seismic activity in earthquake-prone regions was suppressed by the weight of ice sheets [24], leading to increased regional susceptibility to earthquake activity for over 10 000 years following pulses of deglaciation [41]. If such a scenario can be applied to the onset of volcanism and also seismicity in northwestern Africa [5], this would indicate that the Walidiala Valley cap dolostone and Tanagué Member formed within the time frame envisaged for isostatic reequilibration after rapid deglaciation, i.e. 10^3–10^4 [41].

5.4. Possible implications for the snowball-Earth Hypothesis

Our findings above touch on some aspects of the controversial snowball-Earth Hypothesis [20,21]. The snowball-Earth Hypothesis and other published scenarios of Neoproterozoic climate change call for an abrupt end to Elatina–Ghaub–Nantuo glaciation with deglaciation leading to the deposition of cap dolostone units across the world. The major transgression marked by the sharp contact between sandstone of the Tanagué Member and silty dolostone of the Bowal Member is consistent with such an abrupt end to glaciation, and supports the connection between dolomite precipitation and eustatic, deglacial sea-level rise. The transient return to a shallower depositional environment represented by the Tanagué Member is consistent with local continental margin rebound due to the retreat of regional ice shelves and coastal glaciers that presaged more widespread melting of the world's continental ice sheets. Such an interpretation matches the emerging consensus and evidence from the northern Taoudéni Basin [14] that substantial ice sheets existed on the continents during Neoproterozoic glaciations [1] and contradicts the notion that continental ice cover had thinned to nothing by ablation into the world's oceans during total shut-down of the global water cycle [19].

Although dolomite is most commonly a secondary (replacive) carbonate mineral, its growth in the Walidiala Valley cap dolostone in thick seams of volcaniclastic debris that were initially devoid of any carbonate indicates that it may also have precipitated in considerable volumes as a primary mineral during early diagenesis. Early diagenetic porewaters are likely to have been highly oversaturated with respect to dolomite during cap dolostone deposition. Clearly, the saturation state of the ocean changed rapidly during and immediately following deglaciation, possibly within the short 10^3–10^4 year time frame of lithospheric relaxation, a time frame consistent with that envisaged in the Snowball-Earth Hypothesis [20,21]. The abruptness of this change, its apparent association with the injection of alkalinity-poor meltwaters into the world's oceans, and the global scale of the cap dolostone phenomenon mean, however, that this conundrum cannot be solved by the injection of carbonate alkalinity alone through extensive chemical weathering on the continent and associated CO_2 drawdown [20] or from any other point source [37]. Extremely high temperatures [9,10] are also unlikely to have played a major role, considering that cap dolostone O-isotope values are not noticeably different from background dolomite $\delta^{18}O$ values of the Neoproterozoic [38]. It seems to these authors that the required alkalinity must already have existed in the syn-glacial ocean [36] and was supplied to surface waters by mixing of deep syn-glacial brine with the more brackish, surface plume. The precipitation of dolomite in particular may have been

encouraged by the absence of precipitation inhibitors such as sulfate ions related to the buildup of anoxia caused by meltwater-induced ocean stratification [37].

6. Conclusions

The lower part of the Mali Group of the southwestern Taoudéni Basin, northwestern Africa, represents a typical basal Ediacaran-type glaciogenic succession (ca. 635 Ma) with basal debris flows underlying glaciomarine, dropstone-bearing siltstone capped by a regionally extensive, but thin (<6 m) silty dolostone unit that is isotopically indistinguishable from cap dolostone units elsewhere in northwestern Africa and worldwide. A dark debris flow contained in slumps and cavities within the cap dolostone is shown to relate to a volcaniclastic event that was contemporaneous with dolomite cementation of the cap dolostone. The onset of volcanism in this region is probably related to tectonic events in the Panafrican belts, but its prevalence during deglaciation may conceivably have been governed by deglacial, isostatic rebound of the lithosphere. Although seismicity may also have triggered disruption of the cap dolostone and underlying strata, fitted brecciation of the cap dolostone is better explained by dolomite cementation during early diagenesis.

Acknowledgements

We wish to thank Hassanah Diallo, the chief of the village of Tanagué, after whom the Hassanah Diallo Formation is named, for welcoming us to his village in the Walidiala Valley. SJC was supported by National Geographic Society grant No. 3240-85 and National Science Foundation grant No. EAR 8816137. We wish to thank two anonymous experts who provided detailed and useful critique at the review stage. The 2002 field trip was funded by the French CNRS through the ECLIPSE program.

References

[1] P.A. Allen, P.F. Hoffman, Extreme winds and waves in the aftermath of a Neoproterozoic glaciation, Nature 433 (2005) 123–127.
[2] G.H. Barfod, J.D. Vervoort, I.P. Montanez, S. Riebold, Lu-Hf geochronology of phosphates in ancient sediments, Goldschmidt Conference Abstract, Copenhagen, Denmark June 5–11 (2004).
[3] J.-P. Bassot, Étude géologique du Sénégal oriental et de ses confins guinéo-maliens, Mém. Bur. Rech. Géol. Min., Paris 40 (1966) (322 p.).
[4] J. Bertrand-Sarfati, A. Moussine-Pouchkine, B. Amard, A. Aït Kaci Ahmed, First Ediacaran fauna found in western Africa and evidence for an Early Cambrian glaciation, Geology 23 (1995) 133–136.
[5] J. Bertrand-Sarfati, R. Flicoteaux, A. Moussine-Pouchkine, A. Ali Ait Kaci, Lower Cambrian stromatolites and phospharenites related to the glacio-eustatic cratonic rebound (Sahara, Algeria), J. Sediment. Res. 67 (1997) 957–974.
[6] J. Bertrand-Sarfati, A. Moussine-Pouchkine, A. Ali Ait Kaci, Lower Cambrian apatitic stromatolites and phospharenites related to the glacio-eustatic cratonic rebound (Sahara, Algeria), J. Sediment. Res. 67 (1997) 957–974.
[7] G.S. Boulton, M. Deynoux, Sedimentation in glacial environments and the identification of tills and tillites in ancient sedimentary sequences, Precambrian Res. 15 (1981) 322–397.
[8] N. Clauer, M. Deynoux, New information on the probable isotopic age of the Late Proterozoic glaciation in West Africa, Precambrian Res. 37 (1987) 89–94.
[9] S.J. Culver, A.W. Magee, Late Precambrian glacial deposits from Liberia, Sierra Leone, and Senegal, West Africa, Nat. Geogr. Res. 3 (1987) 69–81.
[10] S.J. Culver, D. Hunt, Lithostratigraphy of the Precambrian–Cambrian boundary sequence in the southwestern Taoudéni Basin, West Africa, J. Afr. Earth Sci. 13 (1991) 407–413.
[11] S.J. Culver, J. Pojeta, J.E. Repetski, First record of Early Cambrian shelly microfossils from West Africa, Geology 16 (1988) 599–695.
[12] S.J. Culver, J.E. Repetski, J. Pojeta Jr., D. Hunt, Early and Middle(?) Cambrian metazoan and protistan fossils from West Africa, J. Paleontol. 70 (1996) 1–6.
[13] M. Deynoux, Terrestrial or waterlain glacial diamictites? Three case studies from the Late Precambrian and Late Ordovician glacial drifts in West Africa, Palaeogeogr. Palaeoclimat. Palaeocol. 51 (1985) 97–141.
[14] M. Deynoux, Les formations glaciaires du Précambrien terminal et de la fin de l'Ordovicien en Afrique de l'Ouest. Deux exemples de glaciation d'inlandsis sur une plate-forme stable, Trav Lab. Sci. Terre St-Jérome, Marseille (B) 17 (1980).
[15] M. Deynoux, Periglacial polygonal structures and sand wedges in the Late Precambrian glacial formations of the Taoudeni basin in Adrar of Mauritania (West Africa), Palaeogeogr. Palaeoclimat. Palaeoecol. 39 (1982) 55–70.
[16] D.A.D. Evans, Stratigraphic, geochronological and paleomagnetic constraints upon the Neoproterozoic climatic paradox, Am. J. Sci. 300 (2000) 347–433.
[17] S. Flint, P. Turner, Alluvial fan-delta sedimentation in a forearc extensional setting: the Cretaceous Coloso Basin of northern Chile, in : W. Nemec, R.J. Steel (Eds.), Fan Deltas: Sedimentology and Tectonic Settings, Blackie and Son, Glasgow, UK, 1988 pp. 387–399.
[18] C. Gaucher, P. Sprechmann, Upper Vendian skeletal fauns of the Arroyo del Solado Group, Uruguay, Beringeria 23 (1999) 55–91.
[19] P.F. Hoffman, The break-up of Rodinia, birth of Gondwana, true polar wander and the snowball Earth, J. Afr. Earth Sci. 28 (1999) 17–33.
[20] P.F. Hoffman, A.J. Kaufman, G.P. Halverson, D.P. Schrag, A Neoproterozoic snowball Earth, Science 281 (1998) 1342–1346.
[21] P.F. Hoffman, D.P. Schrag, The snowball Earth hypothesis: testing the limits of global change, Terra Nova 14 (2002) 129–155.
[22] K.-H. Hoffmann, D.J. Condon, S.A. Bowring, J.L. Crowley, U–Pb zircon date from the Neoproterozoic Ghaub Formation, Namibia: constraints on Elatina glaciation, Geology 32 (2004) 817–820.
[23] N.P. James, G.M. Narbonne, T.K. Kyser, Late Neoproterozoic cap carbonates: Mackenzie Mountains, northwestern Canada:

precipitation and global glacial meltdown, Can. J. Earth Sci. 38 (2001) 1229–1262.
[24] A.C. Johnston, Suppression of earthquakes by large continental ice sheets, Nature 330 (1987) 467–469.
[25] A.J. Kaufman, A.H. Knoll, Neoproterozoic variations in the C-isotopic composition of seawater: stratigraphic and biogeochemical implications, Precambrian Res. 73 (1995) 27–49.
[26] M.J. Kennedy, Stratigraphy, sedimentology, and isotopic geochemistry of Australian Neoproterozoic postglacial dolostone: deglaciation, C13 excursions, and carbonate precipitation, J. Sediment. Res. 66 (1996) 1050–1064.
[27] A.H. Knoll, M.R. Walter, G.M. Narbonne, N. Christie-Blick, A new period for the geologic time scale, Science 305 (2004) 621–622.
[28] D.R. Lowe, Sediment gravity flows: II. Depositional models with special reference to the deposits of high-density turbidity currents, J. Sediment. Geol. 52 (1982) 279–297.
[29] J.D. Marshall, Climatic and oceanographic isotopic signals from the carbonate rock record and their preservation, Geol. Mag. 129 (1992) 143–160.
[30] G.V. Middleton, M.A. Hampton, Subaqueous sediment transport and deposition by sediment gravity flows, in : D.J. Stanley, D.J.P. Swift (Eds.), Marine Sediment Transport and Environmental Management, Wiley, New York, 1976, pp. 197–218.
[31] W. Nemec, R.J. Steel, Alluvial and coastal conglomerates: Their significant features and some comments on gravelly-mass-flow deposits, in : E.H. Koster, R.J. Steel (Eds.),Sedimentology of Gravels and Conglomerates, Can. Soc. Petrol. Geol. Mem. 10 (1984) 1–31.
[32] A.C.R. Nogueira, C. Riccomini, A.N. Sial, C.A.V. Moura, T.R. Fairchild, Soft-sediment deformation at the base of the Neoproterozoic Puga cap carbonate (southwestern Amazon craton, Brazil): confirmation of rapid icehouse to greenhouse transition in snowball Earth, Geology 31 (2003) 613–616.
[33] J. Pawlowski, M. Holzmann, C. Berney, J. Fahrni, A.J. Gooday, T. Cedhagen, A. Habura, S.S. Bowser, The evolution of early foraminifera, Proc. Natl Acad. Sci. USA 100 (2003) 11494–11498.
[34] S.M. Porter, A.H. Knoll, P. Affaton, Chemostratigraphy of Neoproterozoic cap carbonates from the Volta Basin, West Africa, Precambrian Res. 130 (2004) 99–112.
[35] G. Postma, Mass-flow conglomerates in a submarine canyon: Abrioja Fan-Delta, Pliocene, southern Spain, in : E.H. Koster, R.J. Steel (Eds.),Sedimentology of Gravels and Conglomerates, Can. Soc. Petrol. Geol. Mem. 10 (1984) 237–258.
[36] A.J. Ridgwell, M.J. Kennedy, K. Caldeira, Carbonate deposition, climate stability, and Neoproterozoic ice ages, Science 307 (2003) 859–862.
[37] G.A. Shields, Neoproterozoic cap carbonates: a critical appraisal of existing models and the plumeworld hypothesis, Terra Nova 17 (2005) 299–310.
[38] G.A. Shields, J. Veizer, Precambrian marine carbonate isotope database: Version 1.1, Geochem. Geophys. Geosyst. 3 (2002) 1031, doi:10.1029/2001GC000266.
[39] R. Trompette, Le Précambrien supérieur et le Paléozoique inférieur de l'Adrar de Mauritanie (bordure occidentale du bassin de Taoudeni, Afrique de l'Ouest). Un exemple de sédimentation de craton, Étude stratigraphique et sédimentologique, Trav. Lab. Sci. Terre St-Jérôme, Marseille (B) 7 (1973).
[40] M. Villeneuve, Etude de la bordure SW du craton ouest-africain, PhD thesis, université Aix–Marseille-3, Marseilles, France, 1984 (552 p.).
[41] P. Wu, P. Johnston, Can deglaciation trigger earthquakes in North America, Geophys. Res. Lett. 27 (2000) 1323–1326.
[42] S. Xiao, Y. Zhang, A.H. Knoll, Three dimensional preservation of algae and animal embryos in a Neoproterozoic phosphorite, Nature 391 (1998) 553–558.
[43] M. Zimmermann, Nouvelle subdivision des séries antégothlandiennes de l'Afrique occidentale (Mauritanie, Soudan, Sénégal), Rap. 21st. Int. Geol. Congr., Copenhagen, vol. 8, 1960, pp. 26–36.